THREE-DIMENSIONAL FRACTOGRAPHY

B. Bauer*, M. Fripan*, and V. Smolej**

The geometric details of fracture surfaces depend on the microstructure of a material, on the fracture behaviour of its constituents and on the mode of loading. An instrumental stereometer allows a relatively fast and accurate measurements of x-y-z coordinates of a large number of selected points in SEM-micrographs of fracture surfaces. Methods for quantifying the three-dimensional geometric characteristic of fracture surfaces are discussed.

INTRODUCTION

Conventional investigations of the fracture surface are usually carried out with individual SEM-micrographs showing the projection of the surfaces and are thus more or less limited to a qualitative interpretation. The stereoscopic method presented here, enables one to obtain profiles from any part and in any direction of the fracture surface (1,2) to describe the topography of the fracture surface by quantitative parameters (grain size, fraction of intercrystalline/transcrystalline crack path, fraction of the constituents, etc.). On the other hand, topographic characteristics not directly related to the microstructure provide valuable information on fracture mechanism. In this paper we aim to show that samples of identical microstructural geometry but different fracture toughness show pronounced differences in fracture topography. For this purpose, we will use the roughness index R_L and the angular distribution of profile segments defined in previous works (3-5).

* Max-Planck-Institut für Metallforschung, Institut für Werkstoffwissenschaften, Stuttgart, FR-Germany

** on leave from Institut "Josef Stefan", Ljubljana, Yugoslavia

EXPERIMENTAL MATERIAL

For demonstration purposes an Al_2O_3-ZrO_2 ceramic has been selected, in which ZrO_2 particles, fine dispersed in the alumina matrix, enhance the fracture toughness of the material. The specimens had the same original microstructure and were both broken at 300 °C in 4-point-bending. The difference between them exists only in the way this temperature has been reached: sample A has been heated from room temperature to the final value, whereas sample B has been cooled down to 300 °C from the starting temperature of 1200 °C. As a result of this treatment the sample B showed a K_{IC} value which was two times higher than the corresponding coefficient for the sample A.

Figs. 1 and 2 show SEM micrographs of both samples at a magnification high enough to make the microstructure visible. The micrographs show the centre of the fracture surface with the observation plane exactly parallel to the loading direction, i.e. perpendicular to the neutral axis. Qualitative observation of the two images does not show any features which were suitable to distinguish between both samples.

DESCRIPTION OF MEASUREMENT

An instrumented stereometer has been developed, which can - when linked to a KONTRON Videoplan computer /1,2/ - be used for measuring three-dimensional coordinates online from stereo-micrographs. This semiautomatic instrument, to be described in detail elsewhere /6/, allows a relatively fast and simple measurement of a large number of x, y, z coordinates. At present up to 500 points can be measured in form of height profiles, height maps or height profiles along irregularly distributed points. This number can easily be increased, although at the sacrifice of speed of measurement.

An obvious advantage of this approach, when compared to the usually practiced method of sample sectioning, is the visibility of the three-dimensional surface being measured. It is easy to select or exclude typical regions of the fracture surface from measurements or to adapt the density of points measured to the surface complexity. Another important advantage of the method is the fact that the sample is not destroyed and that it can be used again, for instance to check the reproducibilty of measurements, or to measure along different profiles etc. It is, however, self-evident, that undercutting details or subsurface cracks can not be detected from pictures of the fracture surface.

Figs. 3-6 show sets of ten profiles (with approx. 50 digitized points each) which have been obtained from stereo-micrographs with help of the stereometer. Profiles have been taken in the region close to the notchground (upper two figures) and in the center of the fracture area (lower two figures). The profiles are perpendicular to the direction of crack propagation and are presented in a way that gives a three-dimensional impression (they are shifted one against each other at a fixed amount both in x and z direction). The scaling is given in mm and is related to the stereo-micrographs.

It is obvious that the final magnification of stereo-pairs will greatly influence the values of parameters chosen for fracture surface characterization. A series of trial tests has shown that the magnification of X400 is best suited for further evaluation of the fracture surfaces studied here. Higher magnification gives no additional imformation. On the other hand, certain surface details, important for fracture processes, are lost at lower magnifications.

PARAMETERS CHARACTERIZING THE FRACTURE SURFACE

In this study we chose the angle distributions of profile elements and the roughness indices R_L - defined as ratios of true profile element lengths against their projections in the plane of measurement - as the parameters that should characterize the fracture surfaces.

a) Angular Distribution

Figs. 7a-10a show the angular distributions of samples A and B, taken in the notchground and in the centre of the fracture surface, respectively. The range of angles is from - 90° to 90°, with a class width of 10°.

The angular distributions, obtained in this way, are hardly to be compared; we suppose that at the magnification used here, the long-range waviness of the samples is not represented statistically in the comparably small measurement area. It is thus present in a form of a curved surface, on which the local roughness of the fracture is superimposed, and therefore leads to erroneous or at least not clearly interpretable angular distributions. To eliminate the unwanted background a polynomial fitting procedure has been performed, which yielded the surface waviness in a form of a trend surface. The residual local roughness which forms a "cleaned" surface, can be analyzed further to obtain distributions.

Figs. 7b-10b present the angular distributions of trend surfaces. Of more interest, however, are figs. 7c-10c, which show angle distributions for "cleaned" surfaces. Here the angular distribution of the notchground for sample B shows symmetrical peaks at $\pm$ 25° (which are already present in uncleaned distributions) and is clearly distinguishable from other distributions which exhibit more or less random characteristics.

b) Roughness Index

The table shows the R_L values calculated from digitized coordinates.

Table - Roughness indices R_L and R_L^* ( ).

	Sample A	Sample B
notch ground	1.28 ± 0.04 (1.27)	1.16 ± 0.02 (1.13)
middle area	1.42 ± 0.06 (1.41)	1.39 ± 0.05 (1.37)

The mean values and standard errors of estimate of R_L have been obtained from 10 profiles measured for each of the fields shown in Figs. 3-6.

Roughness indices seem to be the same for both samples in the centre of the fracture area. However, R_L-values are different, in the notch ground area: the roughness index of the sample with higher K_{IC} is significantly lower. In both samples the surfaces in the center show significantly higher R_L-values as in the area close to the notchground.

The values between brackets in the table present roughness indices R_L^* of "cleaned" surfaces. Comparing R_L and R_L^* we can see that the "cleaning" procedure does not affect the roughness (note that the roughness of the trend surface is nearly 1). Thus we can calculate R_L either from the original or the "cleaned" surface.

CONCLUSIONS

(i) Simple parameters (the linear roughness index and the angular distribution of profile length) are shown to be useful in detecting differences in topography of fracture surfaces.

(ii) The symmetry of the angular distribution is obscured if the projection plane is used as reference. If the inclination and the long-range waviness of the fracture surface are considered by using a trend surface, obtained by polynomial fitting as reference surface, the symmetry of the angular distribution is much better revealed. The linear roughness index is not sensitive to this choice of reference surfaces.

(iii) Differences in fracture toughness of samples with identical microstructural geometries result in pronounced differences of fracture topology in regions close to the notch. Regions further away from the notch do not show significant deviations of roughness or angular distribution between these samples.

(iv) The statistics of the experimental findings are not yet sufficiently established to give a final interpretation of results with respect to fracture mechanisms. Further work in our group is under way to prove the assumption that the different K_{IC}-values of samples A and B are due to the subcritical crack formation in the process zone close to the notch. We hope that this difference can be assessed by quantitative analysis of fracture topography.

REFERENCES

1. Bauer, B.; Haller, A.; Prakt. Met. 18, H7 (1981), 327

2. Bauer, B.; Exner, H.E.; Proc. 3rd. Eur. Symp. Stereol., Ljubljana, Vol. 3, Suppl. 1 (1981), 255

3. Chermant, J.L.; Coster, M.; Journal of Material Science, 14 (1979), 509

4. Pickens, J.R.; and Gurland, J. Fourth International Congress for Stereology, Gaithersburg, Maryland (NBS, Special Publication, (1976), 269

5. Underwood, E.E.; and Underwood, E.S.; Acta Stereol., Proc. 3rd. Eur. Symp. Stereol. 2nd Part, (1982), 89

6. Bauer, B.; Schwarz, H.; to be published

Fig. 2: microstructure of sample B(X2000)

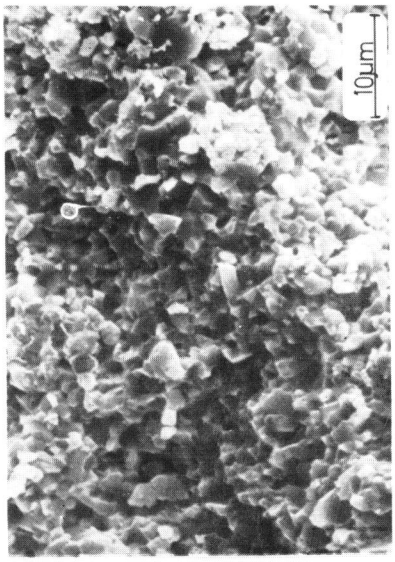

Fig. 1: microstructure of sample A (X2000)

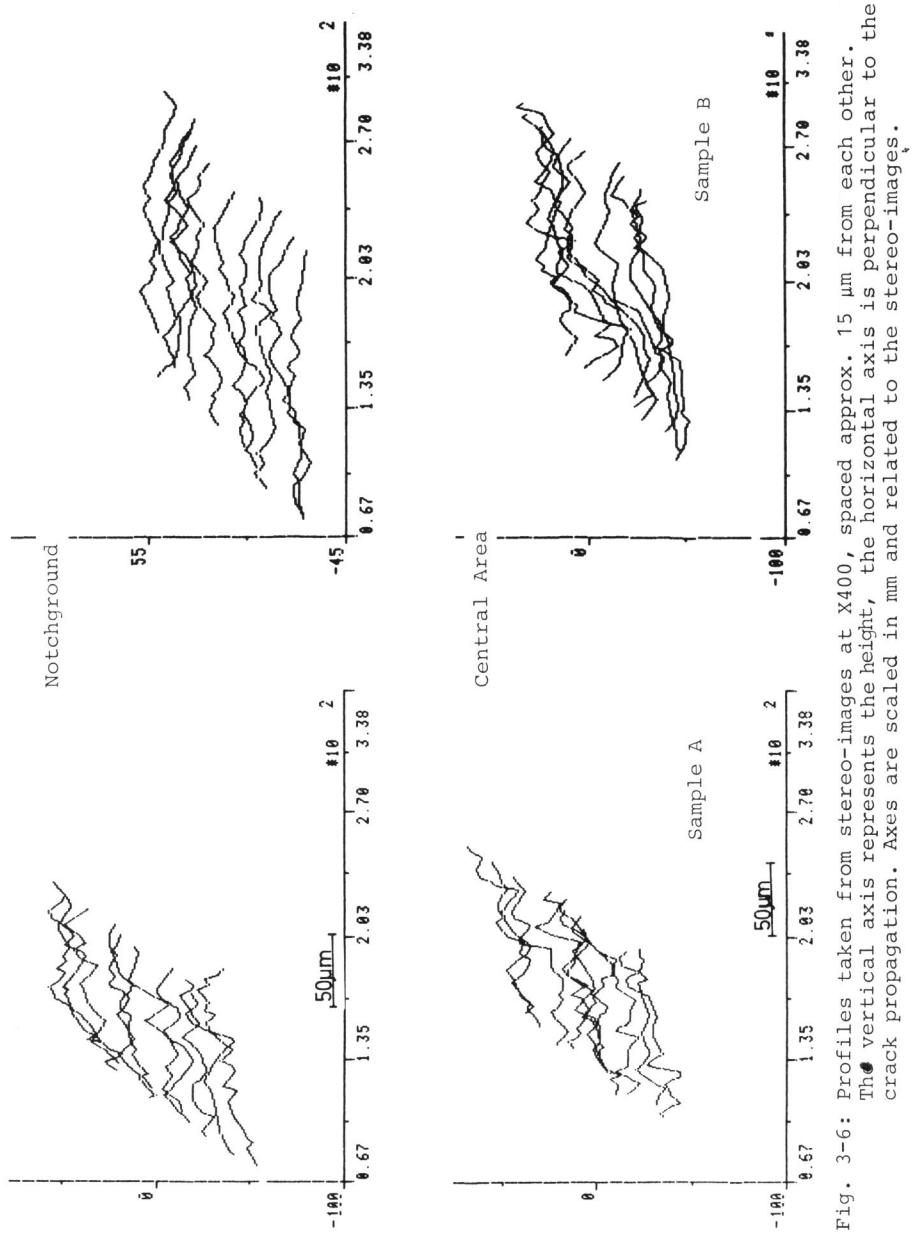

Fig. 3-6: Profiles taken from stereo-images at X400, spaced approx. 15 µm from each other. The vertical axis represents the height, the horizontal axis is perpendicular to the crack propagation. Axes are scaled in mm and related to the stereo-images.

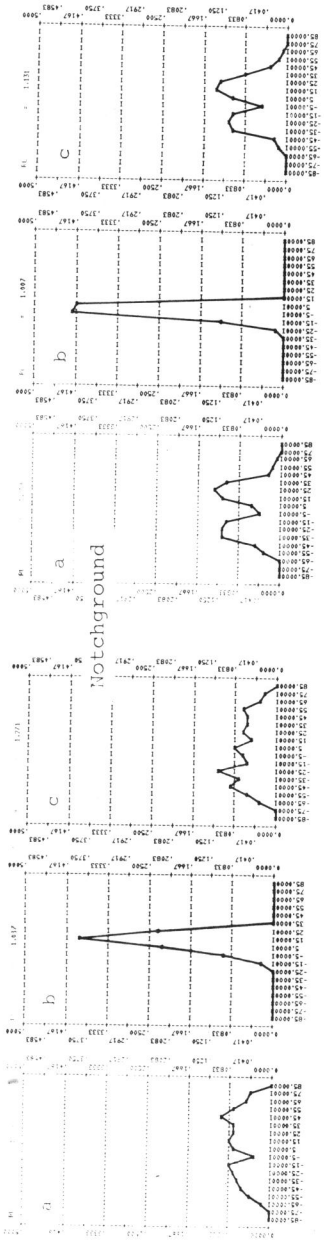

Fig. 7: Sample A

Fig. 8: Sample B

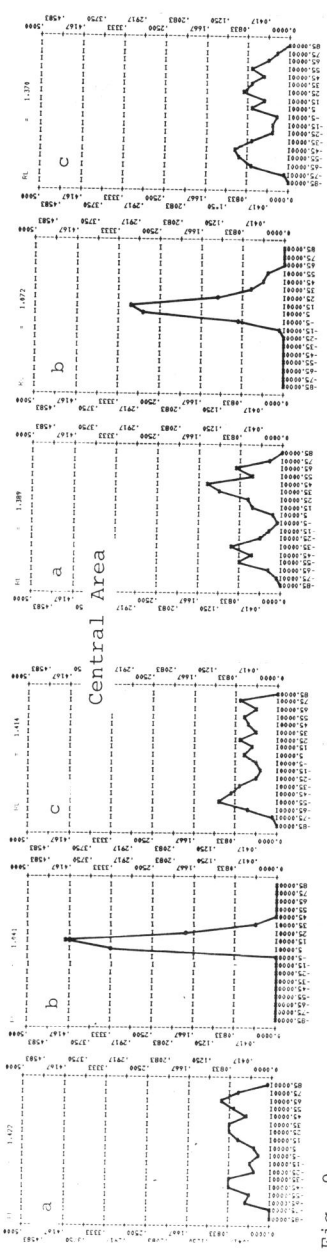

Fig. 9: Central Area

Fig. 10:

Fig. 7-10: Angular distribution of the original profiles from Fig. 3-6(a), from the trend surface (b), and from the residuum (c).